Dilute solution behavior on surface morphology of poly(9-vinylcarbazole)/4,4'-dinitrodibenzyl blends

A. G. GRIGORAŞ[*], V. C. GRIGORAŞ, V. BARBOIU
"Petru Poni" Institute of Macromolecular Chemistry; Grigore Ghica Voda Alley, 41A, Iasi, Romania

Charge transfer (CT) interactions were proved in blends of poly(9-vinylcarbazole) with 4,4'-dinitrodibenzyl (DNDB) in solution and bulk. Besides classical approach to characterization of charge transfer interactions by spectrophotometric methods, here we compare dilute solutions behavior of blends with surface morphology of spin-coated films. Molecular mass and radius of gyration were extracted from MALLS measurements and completed with refractometric measurements. Spin coated blend films were analyzed by AFM and result images shown that their morphology is related to specific interactions between electron-donor PVK and electron-acceptor DNDB. Also, CT interactions are promoted in blend solutions and solid state, too.

1. Introduction

Extensively used as electro-optically active polymer, poly(9-vinylcarbazole) (PVK) has many successful application on xerography [1,2], light-emitting diodes due to his specific photo-physical properties [3-8]. PVK has an saturated hydrocarbon backbone with a helical structure due to aromatic carbazolyl pendants groups. This polymer is a good insulator material with a HOMO (highest occupied molecular orbital) and LUMO (lowest unoccupied molecular orbital) gap of 3.5 eV [9]. Due to the electron-donating property of carbazolyl groups, PVK is largely used as a hole-transport layer in organic light-emitting diodes (OLED) [9-12]. Moreover, the hole conduction inside of PVK can be converted on electron conduction by doping it with other materials based on charge-transfer complexes (CTC) [13,14]. These charge transfer interactions could occur between carbazolyl electron-donor and dinitrobenzoyl electron-acceptor groups, both in polymer-polymer and polymer-low molecular compound systems [15-18].

Miniaturization of electronic devices imposes special morphological features at nanoscale of electronic materials [19,20]. Consequently, many works implied AFM nanolithography [21] or morphological studies on conjugated polymer blends [22,23] and even on PVK. [24, 25]

Behavior of PVK:DNDB blends was compared here both in dilute solution and spin-coated films, based on miscibility of blend components.

2. Experimental

2.1 Materials, Blends and Films Preparation.

PVK (secondary standard from Sigma Aldrich) with average molecular weight Mn of 25000-50000 g/mol and polydispersity index M_w/M_n about 2 was used as received. DNDB synthesis by nitration of the dibenzyl was presented in other work [26]. Based on the chemical structures of PVK and DNDB (figure 1) we roughly exclude other specific interactions such as hydrogen bonding, electrostatic interaction, and Van der Waals types.
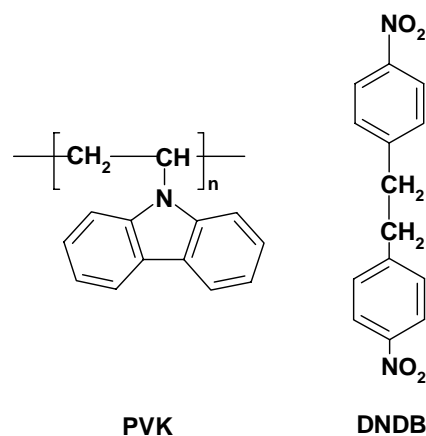

Fig. 1. Chemical structure of PVK and DNDB.

Blends of PVK with DNDB were prepared in chloroform (HPLC grade from Sigma Aldrich). Thus, solutions with 1% wt. concentration were mixed in different PVK:DNDB volumetric ratios (1:5; 1:3; 1:2; 1:1; 2:1; 3:1 and 5:1) and stirred 30 minutes in scintillation vials. In all cases solvent was filtered by 0.02µm filter and stock solutions by 0.45µm Whatman filter.

Spin coating process was extensively used particularly in microelectronics to obtain planar surfaces, many models have been proposed [27-30]. Blend and component solutions were spin coated on mica support at 500 rpm for 1 minute followed by annealing in a vacuum oven for 24h at 70 °C.

2.2 Refractometric measurements

Refractive index increment (dn/dc) was measured at 633 nm and 25 °C, in chloroform with Optilab rEX differential refractometer (Wyatt Technologies) in off-line mode. Sodium chloride (puriss. p.a. for HPLC, Fluka) aqueous solutions were used to instrument calibration.

Based on optical additive-constitutive properties of molecules related to their chemical structure, parameters such as molar refraction and specific volume are useful in material characterization. **Q**uantitative determinations of refraction index and refractive index increment in binary mixtures can deduced by Arago-Biot, Gladstone-Dale, Lorentz-Lorenz, Eykman, Weiner, Heller, Newton, Oster or Eyring-John equations [31].

The dn/dc parameter of polymer depends on concentration, temperature, molecular weight, used wavelength and solvent [32]:

$$dn/dc \approx (n_p - n_s) / \rho_p \qquad (1)$$

where n_p and n_s are the refractive indices of polymer in bulk and the solvent respectively, ρ_p is density of the polymer in the solution. The measurements of this parameter can become complicated in case of multicomponent system. Note that dn/dc for PVK:DNDB solution blends could be considered as function of chemical composition of blend like in a bicomponent system:

$$dn/dc = w_1\,(dn/dc)_1 + w_2\,(dn/dc)_2 \qquad (2)$$

where $w_1 = M_1/(M_1 + M_2)$ and $w_2 = M_2/(M_1 + M_2)$, with M_1, M_2 molar masses of blend components [31, 35].

To measure refractive index increment dn/dc of each blend and components, four solutions with 1.34×10^{-4} to 1.42×10^{-3} g/ml concentration were gravimetrically prepared. Firstly, refractive index increments of PVK and DNDB were determined (0.214 ml/g, respectively 0.157ml/g) and then for different volumetric ratios (1:5; 1:3; 1:2; 1:1; 2:1; 3:1; 5:1).

2.3 Multiangle laser light scattering (MALLS)

MALLS experiments were realized with DAWN DSP laser photometer (Wyatt Technology) in batch mode using scintillation vials at 25 °C. Scattered light intensities were measured at 633 nm, between 14° and 152° to the incident beam. Photometer was calibrated with HPLC-grade toluene (Sigma Aldrich) and detectors were normalized with polystyrene (PL Laboratories). Processing of laser light scattering data and calculations of weight average molecular weight (M_w), root-mean-square radius of gyration (R_G), and second virial coefficient (A_2) were realized by Astra 4.90.07 software. Zimm plots were computed using Berry method, but we eliminated noisy signals of some detectors. The basic equation used to describe light scattering from dilute solutions of macromolecules with dimensions larger than about $\lambda/20$ is:

$$\frac{K \cdot c}{R_\theta} = \frac{1}{M_w P(\theta)} + 2\frac{A_2 c}{P(\theta)} + 3\frac{A_3 c^2}{P(\theta)} \qquad (3)$$

with $K = (2\pi^2 n^2/\lambda^4 N)(dn/dc)^2(1+\cos^2\theta)$ and $P(\theta) = 1-(16\pi^2 n^2 R_G^2/3\lambda^2)\sin^2(\theta\,/2)$, where R_θ is Rayleigh ratio, which is directly proportional to ratio between scattered intensity at angle θ and the incident intensity. K is an optical constant, c is concentration (g/ml) of the scattering species, M_W weight average molar mass, A_2 second virial coefficient, and $P(\theta)$ particle scattering function. In the following calculations, we assume that concentration is sufficiently low to neglect the terms containing the higher virial coefficients than A_2.

2.4 UV-Vis measurements.

Blend solution with concentration in range of 1.34×10^{-5} and 1.73×10^{-4} g/ml allowed us to record UV-Vis absorption spectra using SPECORD 200 Analytik Jena spectrophotometer and 1x1cm² quartz cuvettes.

2.5 AFM Surface analysis

Surface morphology and roughness of coated films were analyzed in air at room temperature using tapping mode with Scanning Probe Microscope (Solver PRO-M, NTMDT, Russia) and NSG10 silicon cantilever (Solver PRO-M, NTMDT, Russia). Cantilever has rectangular shaped and dimensions of approximately 95±5 µm long, 30±5 µm wide and 1.5-2.5 µm thick. The manufacturer's value for probe tip radius is 10 nm and typical force constant is 11.8 N/m. Resonant frequency for this setup was between 236 and 254 kHz. Scan areas were 2x2 µm and 256 x 256 scan point size images were obtained for each sample. Image acquisition and analysis was done by last version of NT-MDT NOVA software.

3. Results and discussion

3.1 Refractometric data.

The calculated values $(dn/dc)^{calc}$ were based on each component contributions to this physical property function of volumetric fraction in blend. Results shown positive or negative deviations of experimental values $(dn/dc)^{633nm}$ compared with $(dn/dc)^{calc}$ values (table 1). These deviations are correlated with CT interaction strength as other authors suggested too [36].

3.2 MALLS measurements.

Same solutions from refractometric measurements were used in static light scattering analysis. To minimize effect of possible errors in low-angle scattering data, a linear fit was preferred. For large-sized random coils, Berry method was used with a linear fit without significant deterioration of the accuracy, unlike the other methods (Zimm or Debye) [37]. Consequently, Berry method was preferred for here, because PVK have random coil conformation in solution. Figure 2 shows Zimm plot analysis (Berry formalism) obtained for 3:1(v:v) PVK:DNDB blend in chloroform at 25 °C, which have same form for all blends.

Table 1. Light scattering and refractometric data for PVK:DNDB blends in chloroform at 25 ^{0}C.

PVK: DNDB (v : v)	PVK in blend (X 10^{-3} g/ml)	M_W (g/mol) (X 10^3)	R_G (nm)	$(dn/dc)^{633nm}$ (ml/g)	$(dn/dc)^{calc}$ (ml/g)
1 : 5	5.0	49.0	102.4	0.162	0.165
1 : 3	7.6	425.5	178.2	0.175	0.169
1 : 2	10.2	18.9	-	0.173	0.174
1 : 1	15.1	137.4	53.9	0.191	0.184
2 : 1	20.7	17.9	-	0.201	0.193
3 : 1	22.7	432.2	90.2	0.196	0.198
5 : 1	25.2	224.9	72.2	0.193	0.202

In accordance with data shown in table 1, the 1:3 and 3:1 blends recorded maximal values of M_W suggesting that CT interactions in solution are most favored at these compositions.

Values of R_G for PVK chain in solution (table 1) have same behavior like M_W function of blend composition.

In almost all blends R_G increases due to molecular motion in solution and chain conformation was changed mainly by charge transfer interactions. Consequently, for a specific volumetric ratio in solution, low-molecular molecules form variable size aggregates with macromolecular chains based on charge transfer.
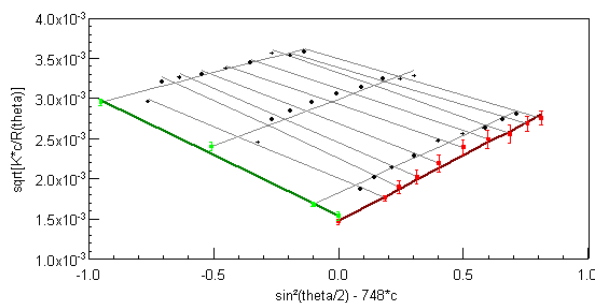
energy between separated counter ions [38]. Usually, UV-Vis spectra recorded on solutions containing electron-donor and electron-acceptor which interact and form charge transfer complex, show beside the bands of blend partners, a new band assigned to charge transfer complex [39,40].
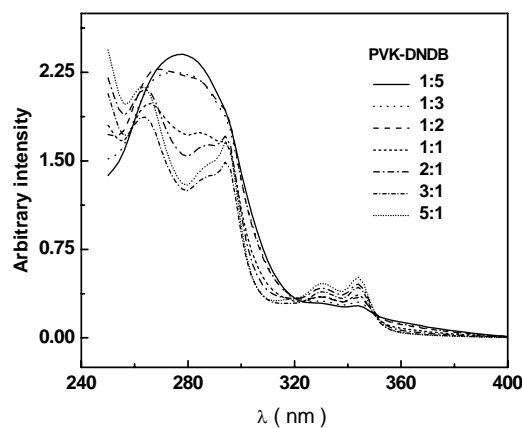

Fig. 3. UV-Vis spectra for PVK:DNDB blends.

Fig. 2. Zimm plot analysis (Berry formalism) for 3:1 blend in chloroform at 25 ^{o}C.

3.3 UV-Vis spectra

Charge transfer depends on ionization potential of donor, electron affinity of acceptor and Coulomb type

Often, even we suppose the nature of interactions between components in the blend, based on intrinsic properties of them, it is possible that the absorption band of CTC being partially or totally shielding by one of the absorption band of partners [41-43].

Similar situation was recorded in our study and results were presented in figure 3. Blends show sharp absorption peaks at 330 nm and 344 nm assigned to carbazolyl group

[44]. Moreover, 1:2 and 1:1 blends recorded a light red shift of PVK maximum absorption from 260 to 270 nm related to stronger CT interactions at these blends compositions.

3.4 AFM results

Some authors investigated the effect of the Hildebrand solubility parameter and vapor pressure of solvents (chloroform, tetrahydrofuran, 1,1,2,2-tetrachloroethane, and N,N-dimehtylformamide) on the microstructure of

PVK film. The high solubility of PVK in chloroform leads to the formation of PVK film with a lower nanotopography [45], so we used that solvent for our blends. Mark-Houwink relationship is related to variation of intrinsic viscosity with molecular weight. For PVK in chloroform the Mark-Houwink exponent falls within 0.5 and 0.8, corresponding to a random coil conformation of polymer [46,47]. Our AFM study was based on fact that initial CT interactions exist on film surface and allow same interactions in bulk, but these depend on chain orientation at film surface and spin-coating process.
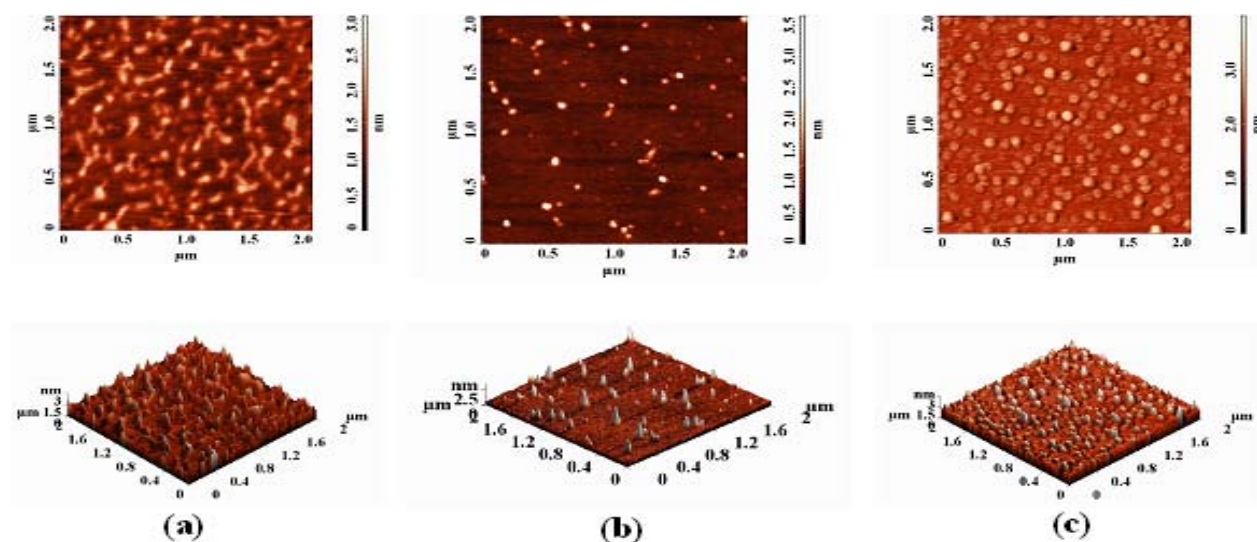

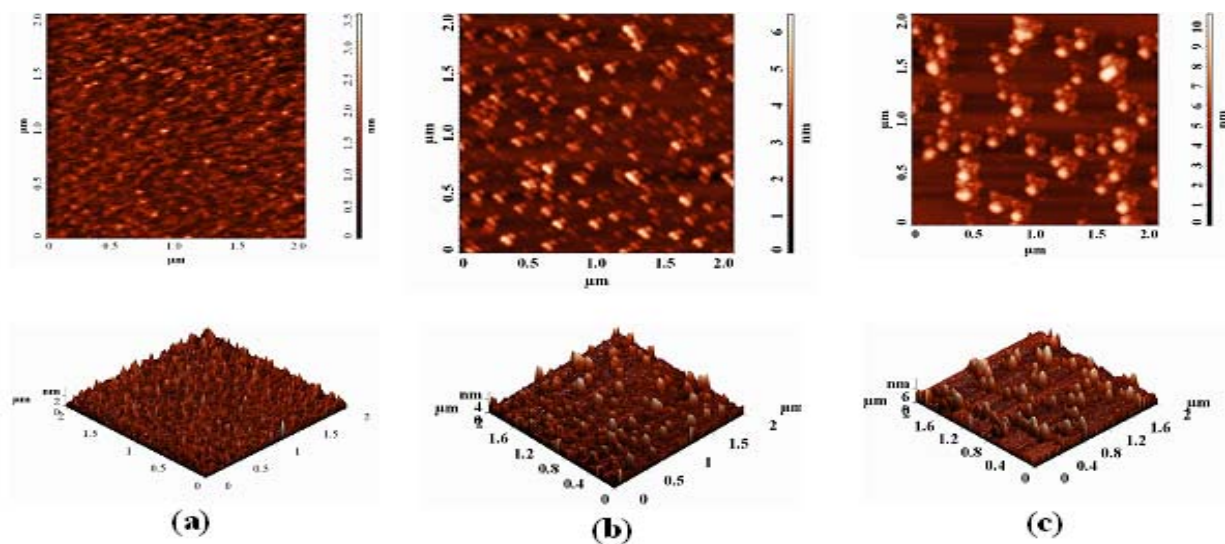*Fig. 4. Tapping-mode AFM images in different volumetric ratio blends: a)1:5; b)1:3; c)1:2.*

Fig. 5. Tapping-mode AFM images in different volumetric ratio blends: a)1:1; b)2:1; c)3:1.
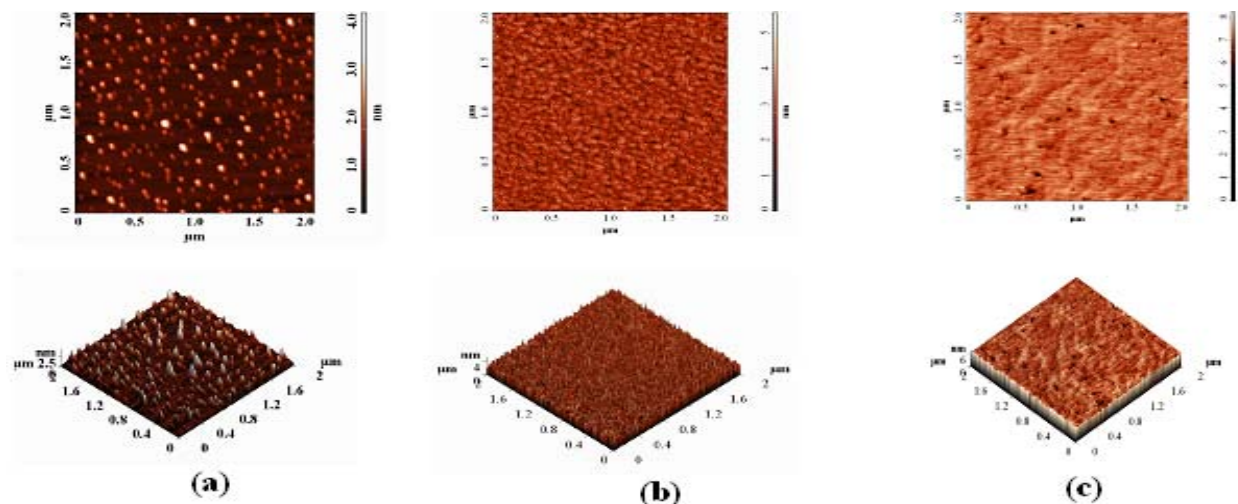
Fig. 6. Tapping-mode AFM images in different volumetric ratio blends: a) 5:1;   b) 1:0;   c)0:1.

For each blend, the tapping-mode (figure 4-6) and phase-contrast AFM images show no indication of phase separation due to immiscible behavior of components. Therefore, in this study, blend films were considered to be homogeneous down to $2x2 \ \mu m^2$ scan areas, so topology were studied close enough to resolution limit of the method [48].

The surface morphology of blends shows different models such as worm-like (1:5 and 1:1 blends similar to PVK), granular surface structure (for 1:2, 1:3, 2:1, 5:1 blends and DNDB) and bead type self-organized domains (3:1 blend). Analyzing blend surface roughness in relation to miscibility between PVK and DNDB, we can say that ordinary miscibility of blend phases explains complexation on neighborhood film surfaces. This miscibility   that is based on CT, influence surface morphology, and lead to complexation as follow: 1:3, 5:1, 2:1 and 3:1. Density of CT interactions for 3:1 blend is higher and allows a surface morphology based on bead-like agglomerations.

4. Conclusions

Experimental refractive index increment values show deviations compared with calculated values for all PVK:DNDB blends. MALLS results sustain refractometric data and consequently CT interactions in solutions were proved.

AFM images of spin coated films shows different surface morphologies depending on blend composition. Carbazolyl groups and nitro substituted benzenic rings promote favorable interactions between PVK and DNDB at surface films.

Behavior in dilute solution have same tendency on surface morphology of spin coated films for all PVK:DNDB blends.

References

[1] J. Y. Moisan, B. André, R. Lever, Chem. Phys. **153**, 305 (1991)
[2] P. M. Borsenberger, D. S Weiss, Organic photoreceptors for xerography. **59,** chapter 8, Marcel Dekker Inc. N.Y. (1998)
[3] L. Valentini, V. Bavastrello, E. Stura, I. Armentano, C. Nicolini, J.M. Kenny, Chem.Phys. Lett. **383**, 617 (2004)
[4] K. Bradley, J.C.P. Gabriel, G. Gruner, Nano. Lett. **3**, 1353 (2003)
[5] M.K. Ram, P. Bertoncello, C. Nicolini, J. Mater. Sci. **38**, 4951 (2003)
[6] Y. Han, G. Wu, H. Chen, M. Wang, J. Appl. Polym. Sci. **109**, 882 (2008)
[7] L.S. Roman, L. Mammo, A.A. Pettersson, M.R. Andersson, O. Inganas, Adv. Mater. **10**, 774 (1998)
[8] Jungwook Han; Jongdeok An; R. N. Jana; Kyungna Jung; Junghwan Do; Seungmoon Pyo; Chan Im.; Macromolecular Research **17**, 894 (2009)
[9] T.D. de Morais, F. Chaput, K. Lahlil, J.-P. Boilor, Adv. Mater. **11**, 107 (1999)
[10] J. Kido, H. Shionoya, K. Nagai, Appl. Phys. Let. **67**, 2281 (1995)
[11] J.-W. Lee, J.-K. Kim, Y.-S. Yoon, Chin. J. Chem. **28**, 115 (2010)
[12] E. Moons, J. Phys. Condens. Matter **14**, 12235 (2002)
[13] W.D. Gill, J.Appl. Phys. **43**, 5033 (1972)
[14] Y. Zhang, Y. Hu, Chen, Q. Zhou, D. Ma, J. Phys. D: Appl. Phys. 36, 2006 (2003)
[15] Y. Shimazaki, M. Mitsushi, S. Ito, M. Yamamoto, Langmuir **13**, 1385 (1997)

[16] Y. Yu, Y. Yao, L. Wang, Z. Li Langmuir
     26, 3275 (2010)

[17] C. Cojocariu, A. Nathansohn, Macromolecules
     36, 2404 (2003)

[18] A. Natansohn, A. Simmons, Macromolecules
     22, 4426 (1989)

[19] U. Durig, G. Cross, M. Despont, U. Drechsler,
     W. Haberle, M.I. Lutwyche, H. Rothuizen, R. Stuts,
     R. Widmer, P. Vettiger, G. K. Binnig, W.P. King,
     K. E. Goodson, Tribol. Lett. **9**, 25 (2002)

[20] W.P. King, T.W. Kenny, K.E. Goodson, G. Cross,
     M. Despont, U. Durig, H. Rothuizen, G.K. Binnig,
     P. Vettiger, Appl. Phys. Let. **78**,1300 (2001)

[21] X.N. Xie, M. Deng, H. Xu, S.W. Yang, D.C. Qi,
     X.Y. Gao, H.J. Chung, C.H. Sow, V.B.C. Tan,
     A.T.S. Wee, J. Am. Chem. Soc. **128**, 2738 (2006)

[22] M. Berggren, O. Inganäs, G. Gustafsson,
     J. Rasmusson, M.R. Andersson, T. Hjertberg,
     O. Wennerström, Nature **372**, 444 (1994)

[23] T.W. Lee, O.O. Park, H.N. Cho, J.-M. Hong,
     C.Y. Kim, Y.C. Kim, Synth. Met. **122**, 437 (2001)

[24] P. Bertoncelloa, A. Notargiacomob, C. Nicolinia,
     Polymer **45**, 1659 (2004)

[25] Y. Yu, Y. Yao, L. Wang, Z. Li, Langmuir
     26, 3275 (2010)

[26] I. Bestiuc, T. Buruiana, G. Caraculacu, V. Popescu,
     Z. Kelemen, A.A. Caraculacu, Rom. Pat.
     85, 582 (1982)

[27] A.G. Emslie, F.T. Bonner, L.G. Peck, J. Appl. Phys.
     29, 858 (1958)

[28] D. Meyerhofer, J. Appl. Phys. **49**, 3993 (1978)

[29] W.W. Flack, D.S. Soong, A.T. Bell, L.E. Hess,
     J. Appl. Phys. **56**, 1199 (1984)

[30] C.J. Lawrence, Phys. Fluids **31**, 2786 (1988)

[31] S. Sharma, P.B. Patel, R.S. Patel, J.J. Vora, e-Journal
     of Chemistry **4**, 343 (2007)

[32] J. Carlfors, R. Rymden, Eur. Polym. J. **18**, 933 (1982)

[33] I. Teraoka, Polymer solutions, chapter 2, p.130,
     John Wiley & Sons Inc. (2002)

[34] A. Noor, A. Sabz, Coll. Polym. Sci. **256**, 1085 (1978)

[35] B. Coto, J.M. Escola, I. Suarez, M.J. Caballero,
     Polymer Testing **26**, 568 (2007)

[36] R. Sahai, V. Singh, Bull. Chem. Soc. Jpn.
     53, 1785 (1980)

[37] M. Andersson, B. Wittgren, K.G. Wahlund,
     Analytical Chemistry **75**, 4279 (2003)

[38] C. Wang, Z.X. Guo, S. Fu, W. Wu, D. Zhu, Prog.
     Polym. Sci. **29**, 1079 (2004)

[39] H. Duymus, M. Arslan, M. Kucukislamoglu,
     M. Zengin, Spectrochimica Acta **A65**, 1120 (2006)

[40] R. Foster, Charge-transfer complexes,
     vol.51, Academic Press, London (1969)

[41] C.R. Patrick, G.S. Prosser, Nature **187**, 1021 (1960)

[42] J. H. Williams, J. K. Cockcroft, A. N. Fitch,
     Angewandte Chemie **104**, 1666 (1992)

[43] H. Gregorius, M. Baumgarten, R. Renter, K. Müllen,
     N. Tyutyulkov, Angew. Chem. Int. Ed. Engl.
     31, 1655 (1992)

[44] J.H. Park, O.O. Park, J. Kim, J.W. Yu, J.K. Kim,
     Y.C. Kim, Curr. Appl. Phys. **4**, 659 (2004)

[45] U. Paik, S. Lee, J.G. Park, J. Semicond. Techn. Sci.
     8, 46 (2008)

[46] G. Sitaramaiah, D. Jacobs, Polymer **11**, 165 (1969)

[47] S.-C. Luo, V. Craciun, E.P. Douglas, Langmuir
     21, 2881 (2005)

[48] R. Stevenson, R. Riehn, R.G. Milner, D. Richards,
     M. Moons, D.-J. Kang, M. Blamire, J. Morgado,
     F. Cacialli, Appl. Phys. Lett. **79**, 833 (2001)

_____
[*]Corresponding author: angrig@icmpp.ro